A new procedure for measuring the decohesion energy for thin ductile films on substrates

A. Bagchi, G. E. Lucas, Z. Suo, and A. G. Evans
Materials Department, College of Engineering, University of California–Santa Barbara, Santa Barbara, California 93106-5050

(Received 15 July 1993; accepted 24 March 1994)

A novel testing technique has been developed capable of measuring the interfacial fracture resistance, Γ_i, of thin ductile films on substrates. In this technique, the thin film on the substrate is stressed by depositing onto the film a second superlayer of material, having a large intrinsic stress, such as Cr. Subsequent processing defines a precrack at the interface between the film and the substrate. The strain energy available for driving the debond crack is modulated by varying the thickness of the Cr superlayer. Spontaneous decohesion occurs for superlayers exceeding a critical thickness. The latter is used to obtain Γ_i from elasticity solutions for residually stressed thin films. The technique has been demonstrated for Cu thin films on silica substrates.

I. INTRODUCTION

The decohesion of interfaces between metals and nonmetals is a critically important technological issue.[1,2] Many of the basic phenomena have been identified, particularly the role of the interface debond energy, Γ_i, and its dependence on the loading mixity, Ψ (Fig. 1).[3,4] The latter is a measure of the relative shear to tensile opening of the interface crack surfaces near the tip. Methods for measuring Γ_i have also been devised and calibrated (Fig. 2).[4–6] However, these methods typically require specimens made by using a high homologous temperature (T/T_m) processing step, such as the diffusion bonding of sandwich specimens: T and T_m denote the processing temperature and the metal melting point, respectively (Fig. 2). For interfaces that have experienced only low temperatures upon fabrication, there are many tests for the qualitative ranking of the interface fracture resistance. These include scratch,[7] microscratch,[8,9] peel,[10,11] and blister tests.[12,13] However, the full quantification of most of these tests has not usually been possible because of the complex elastic/plastic stress fields involved. For example, models for the microscratch test[9] are based on simplifying assumptions regarding the stress state and the decohered area. One exception is the peel test, which has been quantified.[10,11] Even then, deconvolution of Γ_i from the peel force is complex and subject to appreciable uncertainties. Moreover, this test has a mode mixity that differs in sign and magnitude from that associated with most practical decohesion problems.[3] Blister tests are more readily interpreted but also provide mode mixities having inappropriate sign.[12,13] Such tests have further limitations when applied to thin, opaque, ductile films. There are two practical problems. The pressure imposed to induce decohesion increases the stress in the film and may cause yielding. Moreover, the perimeter of the decohered zone is difficult to measure. A preferred test method for ductile films would be one in which the stresses in the film diminish as the decohesion extends and also have an energy release rate G independent of the decohered length.

The present article addresses the deficiencies by devising a new test that has the following attributes. The method can be used for ductile thin films deposited onto substrates at low T/T_m. It has a mode mixity typical of that associated with thin film decohesion ($\Psi \approx 0°$–$50°$) and G independent of decohesion length. Moreover, the

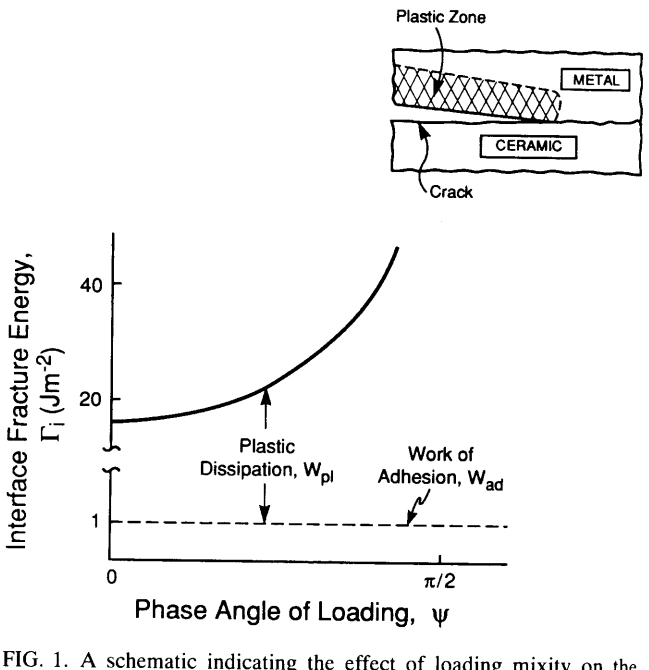

FIG. 1. A schematic indicating the effect of loading mixity on the interface fracture energy, Γ_i. The values used are typical for metal/oxide interfaces. Also shown is a schematic of crack growth with plastic dissipation.

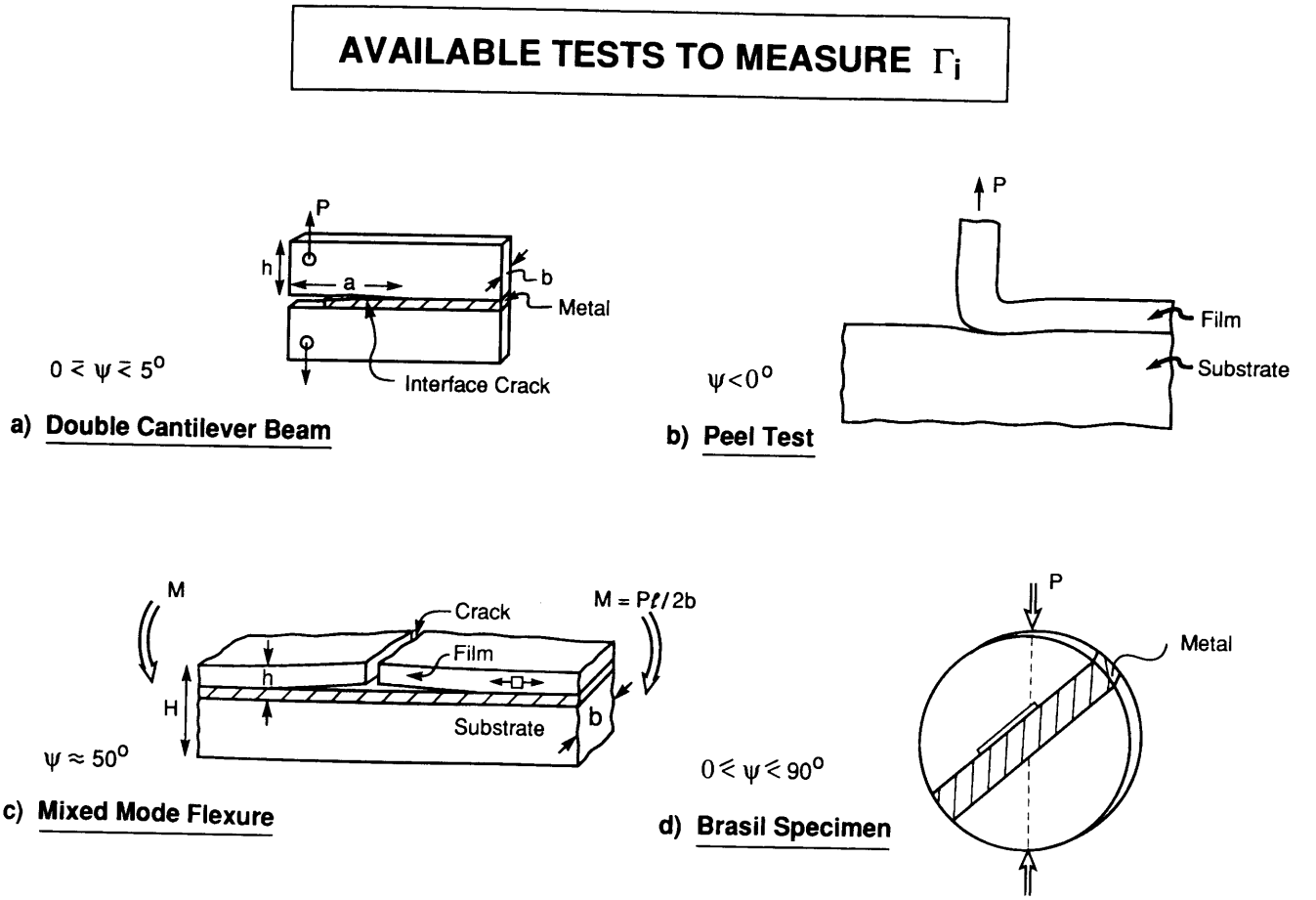

FIG. 2. Some test methods used to measure the interface fracture energy.

stress in the film decreases as decohesion proceeds. The procedure can also be implemented in a conventional microelectronics fabrication facility.

Interface decohesion occurs subject to several dissipation mechanisms.[14–16] The fundamental mechanism involves the work of adhesion, W_{ad}, which represents the basic separation energy for the bonds across the interface. In general, plastic dissipation W_{pl} also occurs within a plastic zone in the metal, as the decohesion extends along the interface (Fig. 1). This contribution scales with W_{ad}.[15,16] It also varies with crack extension, Δa, leading to a resistance curve.[16] This curve, in turn, depends on the ratio of the peak decohesion stress, $\hat{\sigma}$, to the yield strength of the metal, σ_0 (Fig. 3). Moreover, W_{pl} may increase as the film thickness becomes larger and as the mode mixity angle increases (Fig. 1). In some cases, when the interface is nonplanar, frictional effects can also contribute to Γ_i.[3] The new test method has been devised with the intent of systematically exploring these effects for metal thin films on nonmetallic substrates.

II. SOME BACKGROUND MECHANICS

The relevant mechanics of thin film decohesion consider a thin film subject to residual tension, σ_f, on a thick substrate (Fig. 4). The energy release rate associated with an interface decohesion, originating from an edge (or discontinuity), attains a steady-state value, G_{ss}, provided that the decohesion length, a_0, exceeds the film thickness. Moreover, since all of the stress in the film

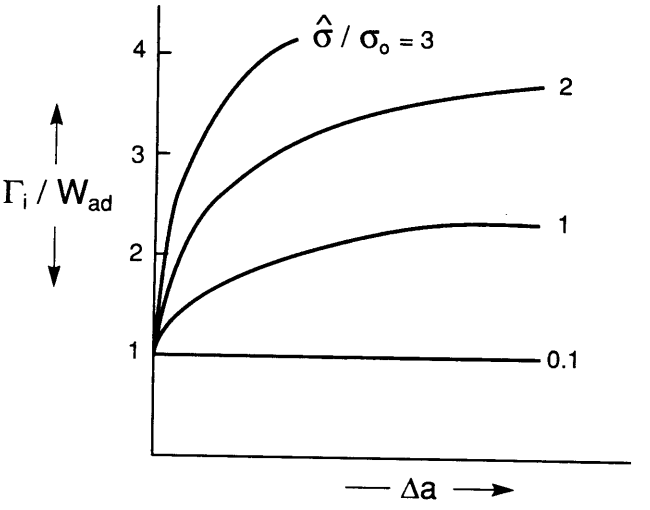

FIG. 3. Effect of metal yield strength on the interface fracture energy: σ_0 is the yield strength, $\hat{\sigma}$ the bond strength, and Δa the crack extension.[16]

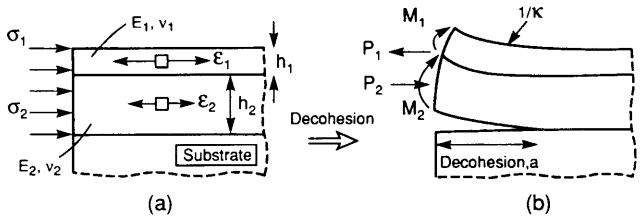

FIG. 4. A schematic showing the behavior of a bilayer film subject to residual tension as it decoheres from the substrate. The stresses σ_1 and σ_2 (a) are the misfit stresses, which provide the forces P_i and the moments M_i (b) in the metal bilayer above the decohesion crack. The curvature of the decohered bilayer film is κ.

above the decohesion is released, the nondimensional energy release rate for a thin strip is[3,17]

$$G_{ss}E_f/\sigma_f^2 h_f = 1/2, \tag{1}$$

where E_f is Young's modulus for the film and h_f is the film thickness. The corresponding mode mixity is $\Psi = 52°$. The thin film test method should duplicate this mode mixity. For a wide strip (width $w > h_f$), the residual stresses are biaxial and the revised steady-state energy release rate is[3]

$$G_{ss}E_f/\sigma_f^2 h_f = 1 - \nu_f, \tag{2}$$

where ν_f is Poisson's ratio of the film. At smaller decohesion lengths ($a_0 < h_f$), the energy release rates depend on the details at the edge.[3,17] The preferred test method should avoid these edge problems by using only decohesion precracks within the steady-state range.

For a bilayer film, interface decohesion leads to bending, whereupon some energy is stored in the film above the decohesion. Consequently, the steady-state energy release rate is reduced. The new value, as derived in the Appendix, is

$$G_{ss} = \sum_i \frac{\sigma_i^2 h_i}{E_i'} - \sum_i \frac{1}{E_i'}\left[\frac{P^2}{h_i} + \frac{12M_i^2}{h_i^3}\right], \tag{3}$$

where $i = 1, 2$ refer to the two materials in the bilayer. The load P associated with the residual tension σ_i in each layer (Fig. 4) can be expressed in terms of the curvature of the decohered bilayer, κ, the film thickness, h_i, and the biaxial elastic moduli, $E_i' = E_i/(1 - \nu_i)$, as[18]:

$$P = \left[\frac{E_1'h_1^3 + E_2'h_2^3}{6(h_1 + h_2)}\right]\kappa \tag{4}$$

with κ given by

$$\kappa = \frac{6(h_1 + h_2)(\varepsilon_1 - \varepsilon_2)}{[h_1^2 + E_2'h_2^3/E_1'h_1 + E_1'h_1^3/E_2'h_2 + h_2^2 + 3(h_1 + h_2)^2]}, \tag{5}$$

where $\varepsilon_i = \sigma_i/E_i'$. The bending moment, M_i (**Fig. 4**), is given by

$$M_i = E_i'\kappa, \tag{6}$$

where I_i is the moment of inertia, $I_i = h_i^3/12$.

III. THE METHOD

A key consideration for development of a method concerns the mode mixity, Ψ. In order to maintain Ψ in the requisite range, there are few options for loading the system. Among these, the only approach that appears to be straightforward involves the use of a residual stress which essentially duplicates the problem of interest. However, for typical thin films ($h_f < 1$ **μm**), and representative residual stress levels ($\sigma_f^R < 100$ **MPa**), the residual stress-induced energy release rate is small [Eq. (1)], of the order, $G_{ss} \approx 0.1$ Jm^{-2}. Most interfaces with practical interest would have a debond energy substantially larger than this.[14] Consequently, decohesion would not be induced. The preferred test method must identify a procedure that substantially increases G_{ss}, without changing Ψ, while also preserving the structure and microstructure of the interface.

A method that increases the energy release rate, at essentially constant Ψ, involves deposition of an additional material layer onto the film. This superlayer increases the total film thickness and also elevates the total residual stress without changing the interface. In order to accomplish this, the additional layer must be deposited in accordance with the following three characteristics. Deposition must be conducted at ambient temperature. The layer must not react with the existing film. The layer must have a large residual tension upon deposition. A Cr film, deposited by electron beam evaporation, meets all three criteria.[19]

The new test method has the following three features: (i) A decohesion precrack is created, with length $a_0 > h_f$. (ii) The film is patterned to form narrow strips. (iii) The Cr film thickness is varied in order to produce a range of energy release rates. To provide these features, a thin strip of carbon is first deposited. This layer is the source of the interface precrack (Fig. 5). The film of interest is then deposited. Subsequently, a Cr layer with the requisite thickness is deposited onto the film. Thereafter, the bilayer is patterned to form strips orthogonal to the carbon lines. Finally, the strips are severed above the C. The latter step creates the edge needed to induce an energy release rate (Fig. 5). The half-width of the carbon line, a_0, defines the precrack length. When the strips decohere after severing, the energy release rate exceeds the debond energy; i.e., $G_{ss} > \Gamma_i$. Conversely, when the film remains attached, $G_{ss} < \Gamma_i$. Consequently, Γ_i is determined from the critical Cr layer thickness above

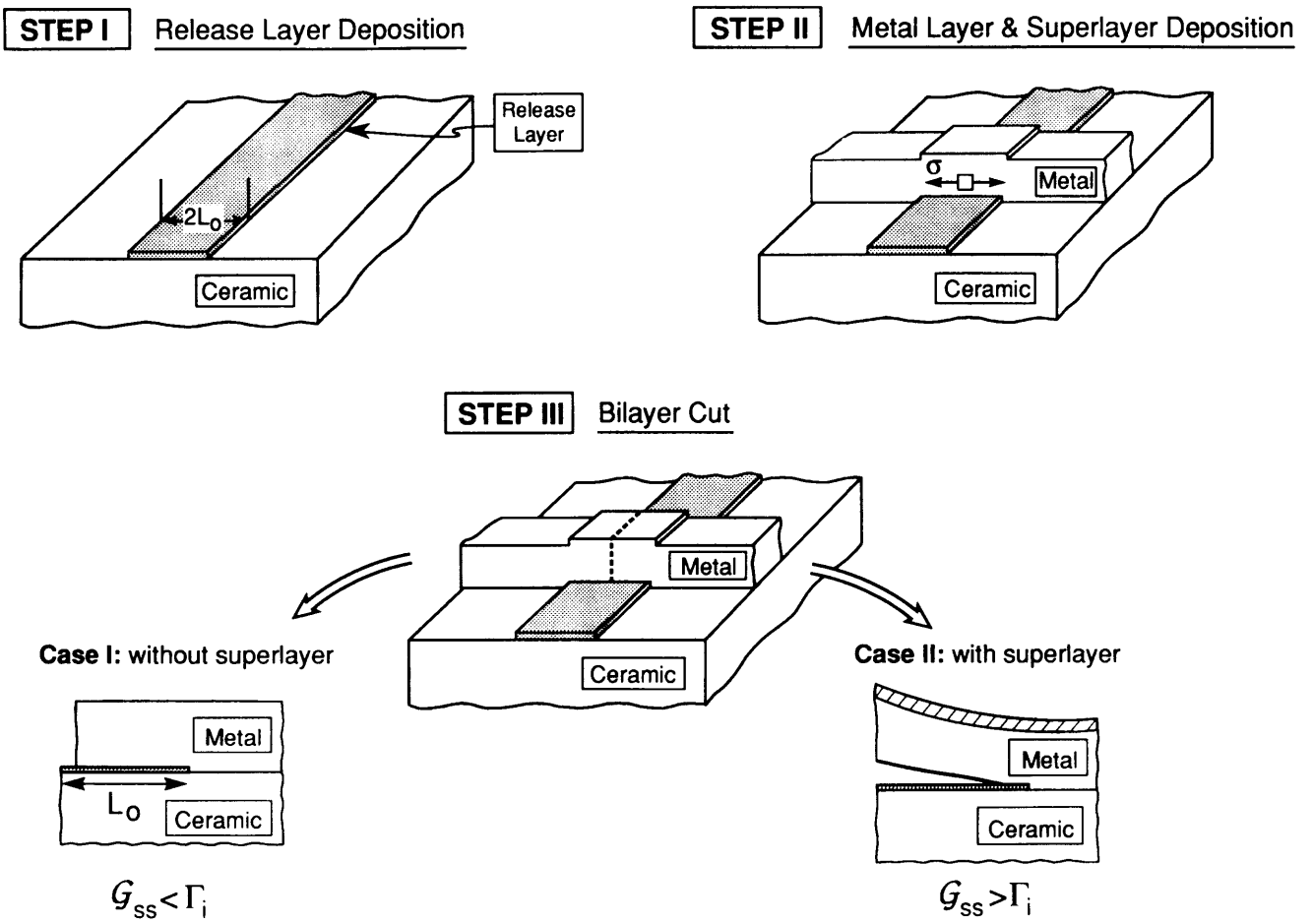

FIG. 5. The procedure used to measure the debond energy of the interface.

which decohesion always occurs, designated h_c. The bilayer solution [Eq. (3)] then relates Γ_i to the critical Cr thickness by using the equalities: $G_{ss} = \Gamma_i$ and $h_1 = h_c$.

IV. EXPERIMENTAL PROCEDURE

A flow chart of the overall procedure is presented in Fig. 6. Deposition and photolithography are conducted in a clean room facility. Residual stresses are measured from beam deflections. Then, film severing above the precrack is conducted. The films are inspected to assess the critical thickness, h_c. Finally, this critical thickness is used to determine Γ_i.

A. Deposition and patterning

Preliminary experiments have been carried out by using evaporated copper films and glass substrates. The choice of copper is particularly attractive due to its emerging importance as an interconnect material. It is expected to replace aluminum for deep submicron metal linewidths, because of its superior conductivity and higher resistance to electromigration.[20] All processing steps are carried out in Class 100 and Class 10 000 clean room facilities. Careful substrate cleaning is essential. For this purpose, the glass substrates (Corning 0211) are solvent cleaned in trichloroethylene, acetone, and isopropyl alcohol in order to remove organic contaminants. Then, they are water cleaned, followed by etch-cleaning in buffered hydrofluoric acid, in order to remove all inorganic contaminants. Finally, they are rinsed in de-ionized water and dried. The carbon release layer is thermally evaporated (thickness ~200 Å) onto the substrate and patterned to the desired geometry (Fig. 5) by using a bilayer photolithography technique. Pure copper (99.999%) is then deposited by electron beam evaporation at a background pressure $\approx 8 \times 10^{-7}$ Torr. Thereafter, the chromium superstructure layer (99.9% pure) is evaporated. An *in situ* quartz monitor is used to control the deposition rate (Cu ~10 Å/s, Cr ~1 Å/s) and the film thickness. Subsequent lift-off defines the metal line geometry. Finally, a through cut is made in the metal bilayer by wet etching. An optical micrograph of a processed test specimen is shown in Fig. 7.

B. Residual stress measurement

The residual stress is measured by using a standard procedure that relies on determination of the

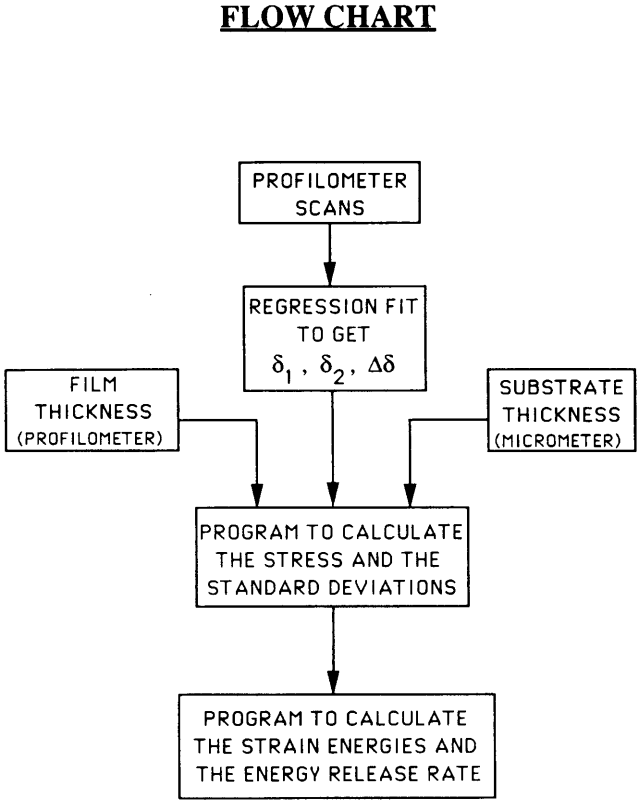

FIG. 6. A flow chart indicating the sequence used to measure the debond energy.

film/substrate system.[21] For this purpose, a profilometer is used to measure substrate curvature.[22] The profilometer uses a metallic stylus, which is horizontally scanned while its vertical movement is converted to an electrical signal. The substrate often has an initial curvature. Therefore, two scans are made in order to measure the bending deflection of the substrate. These are made both with (δ_1) and without (δ_2) the film attached. The residual stress in the film is related to these displacements by:

$$\sigma^R = \frac{4E_s(\delta_1 - \delta_2)h_s^2}{3(1 - \nu_s)L^2h_f}, \tag{7}$$

where L is the length of the profilometer scan, h_s is the substrate thickness, and E_s, ν_s are the substrate Young modulus and Poisson's ratio, respectively. This procedure is used to evaluate the residual stress in the Cu and then the residual stress in the Cr deposited onto the Cu. The total stress, σ_{tot}, associated with both is

$$\begin{aligned}\sigma_{tot} &= \sigma_{Cr}H_{Cr} + \sigma_{Cu}H_{Cu} \\ &= \sigma_{Cu} + (\sigma_{Cr} - \sigma_{Cu})H_{Cr}\,,\end{aligned} \tag{8}$$

where H is the relative layer thickness,

$$H = h/(h_{Cu} + h_{Cr})\,.$$

Consequently, if the stresses are essentially independent of the film thicknesses, there would be a linear dependence of the total stress on the relative thickness, H. This approach is used to assess the experimental results.

V. RESULTS

A. Residual stress

Residual stress measurements have been performed on a batch of four samples with the same nominal Cu thickness (4425 Å) and with four Cr thicknesses: 220 Å, 445 Å, 660 Å, and 900 Å. On each sample, five profilometer scans were made before and after removing the film from the substrate. A least square regression fitting to the data gives the deflections (δ_1 and δ_2) and their respective standard deviations. The film thickness is also obtained from the scans. The substrate thickness is measured with a digital micrometer. The stresses obtained in this manner are plotted in Fig. 8. A linear fit appears to obtain, consistent with stresses in each separate layer being independent of thin film thickness

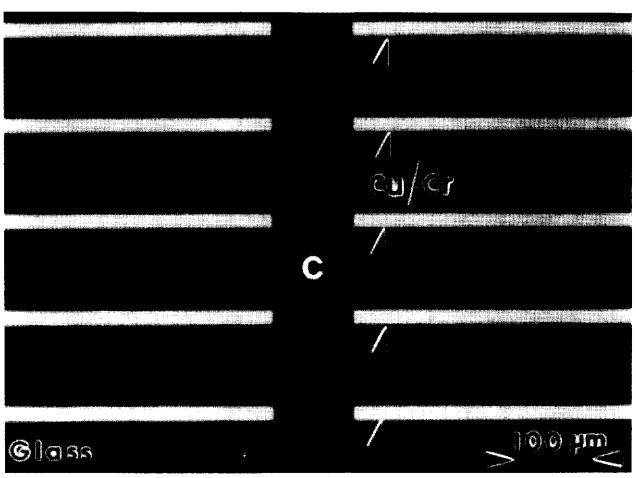

FIG. 7. An optical micrograph of the processed test specimen.

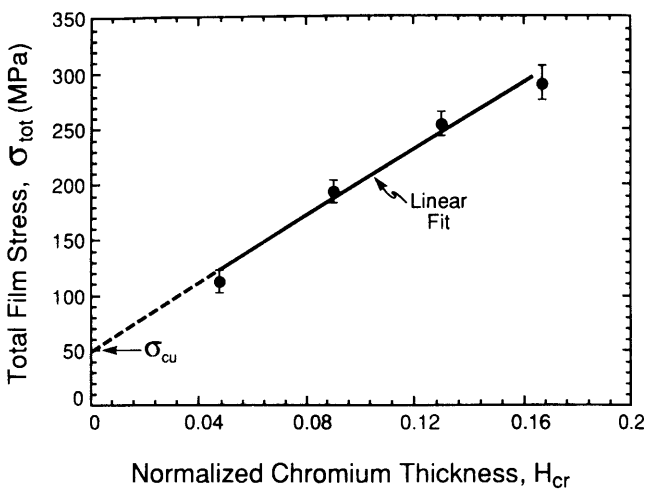

FIG. 8. A plot of the total film stress with the normalized Cr layer thickness.

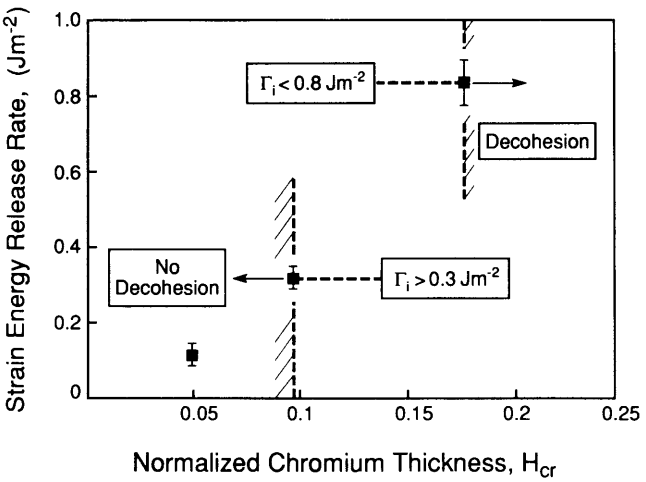

FIG. 9. A plot of the calculated energy release rates with the normalized Cr layer thickness. Also shown are the lines separating the film that decohered from that which remained attached and associated bounds in the interface fracture energy.

[Eq. (8)]. This fit indicates that the residual stresses in the Cu and Cr layers are 50 MPa and 1575 MPa, respectively, with standard deviations ~3%. The former is consistent with the yield strength of Cu films, and both values are within the range measured by others.[23]

B. Interfacial fracture energy

For a glass substrate with a 0.44 μm thick Cu film, the results are summarized in Fig. 9. When the Cr superlayer was either 22 nm or 45 nm thick, the bilayer remained attached to the substrate (Fig. 10(a)). Conversely, when the Cr layer was 90 nm thick, decohesion occurred, followed by curling of the film (Fig. 10(b)). Consequently, h_c is between 45 nm and 90 nm. By introducing these values into the energy release rate formula for the bilayer [Eq. (3)], bounds are placed on the interface fracture energy. For this purpose, the elastic modulus of the film is needed. Generally, polycrystalline thin films can have a lower modulus than the bulk material, because of porosity at the boundaries of the columnar grains. Consequently, for completeness, independent measurement of E_f would be needed. Such measurements have yet to be performed in this study. Instead, literature values of polycrystalline Cu and Cr thin films are used (E_f = 120 GPa[24] and 93 GPa,[25] respectively). With these choices for E_f, the bounds on the interface fracture energy are $0.3 \leqslant \Gamma_i \leqslant 0.8$ Jm^{-2}. Earlier study of Cu/glass interfaces, produced by diffusion bonding and annealing, indicated that Γ_i usually ranged between 0.14 and 4 Jm^{-2} (the highest being 8 Jm^{-2}).[26] The scatter was attributed to surface contaminants, which influenced the bonding. The present results are at the lower end of this range. Such results are consistent with the absence of an annealing step, in the present study, leading to a more pronounced influence of minor contaminants. These, in turn, reduce the potential for a contribution to Γ_i from plastic dissipation in the Cu. The present values are comparable with the work of adhesion (W_{ad} = 0.5 Jm^{-2}) for liquid Cu on SiO_2.[27] This suggests that there is a minor contribution to Γ_i from plastic dissipation, perhaps because the Cu film is relatively thin.

VI. CONCLUDING REMARKS

A new test procedure for measuring the interface decohesion energy Γ_i of metallic thin films on nonmetallic substrates has been devised, analyzed, and demonstrated. The procedure duplicates the conditions found upon decohesion induced by residual stress. The measured values of Γ_i may thus be used directly, in conjunction with the mechanics of thin films in order to predict such factors as the critical film thickness. Moreover,

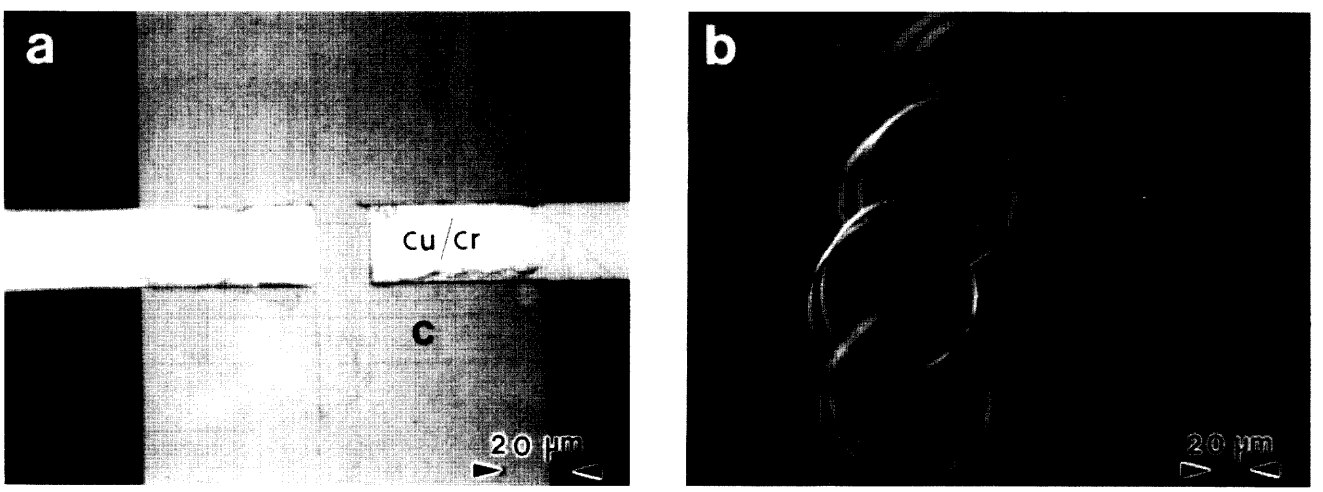

FIG. 10. Specimens providing the lower and upper bounds in the fracture energy, with the Cr superlayer thickness (a) h_1 = 450 Å, below the critical thickness, and (b) h_1 = 900 Å, above the critical thickness.

the method allows a systematic study of trends in Γ_i with the key deposition and postdeposition variables. These include the effect of contaminants, of active metal layers, of annealing, electric fields, etc. Studies are now in progress which will apply the new method to these basic issues.

Finally, since the value of Γ_i obtained from these tests is subjected to knowledge of the elastic properties of the bilayer film, simple acoustic procedures for measuring these properties are being implemented.

ACKNOWLEDGMENT

Financial support was provided by the Office of Naval Research under ONR Contract N00014-93-I-0213.

REFERENCES

1. P.S. Ho, Appl. Surf. Sci. **41–42**, 559 (1989).
2. M.D. Thouless, J. Vac. Sci. Technol. A **9**, 2510 (1991).
3. J.W. Hutchinson and Z. Suo, Adv. Appl. Mech. **29**, 63 (1992).
4. A.G. Evans, M. Rühle, B.J. Dalgleish, and P.G. Charalambides, Metall. Trans. **21A**, 2419 (1990).
5. P.G. Charalambides, J. Lund, A.G. Evans, and R.M. McMeeking, J. Appl. Mech. **56**, 77 (1989).
6. J.S. Wang and Z. Suo, Acta Metall. Mater. **38**, 1279 (1990).
7. J. Ahn, K.L. Mittal, and R.H. MacQueen, *Adhesion Measurement of Thin Films, Thick Films, and Bulk Coatings*, ASTM STP 640, edited by K.L. Mittal (American Society for Testing and Materials, 1978), p. 134.
8. T.W. Wu, J. Mater. Res. **6**, 407 (1991).
9. S. Venkataraman, D.L. Kohlstedt, and W.W. Gerberich, J. Mater. Res. **7**, 1126 (1992).
10. K-S. Kim and N. Aravas, Int. J. Solids Struct. **24**, 417 (1988).
11. K-S. Kim and J. Kim, J. Eng. Mat. Tech. **110**, 266 (1988).
12. M.G. Allen and S.D. Senturia, J. Adhesion **25**, 303 (1988).
13. M.G. Allen and S.D. Senturia, J. Adhesion **29**, 219 (1989).
14. A.G. Evans and B.J. Dalgleish, Acta Metall. Mater. **40**, Suppl., S295 (1992).
15. M.L. Jokl, V. Vitek, and C.J. McMahon, Jr., Acta Metall. Mater. **28**, 1479 (1980).
16. V. Tvergaard and J.W. Hutchinson, J. Mech. Phys. Solids **41**, 1119 (1993).
17. M.D. Drory, M.D. Thouless, and A.G. Evans, Acta Metall. Mater. **36**, 2019 (1988).
18. S. Timoshenko, J. Opt. Soc. Am. **11**, 223 (1925).
19. M.S. Hu and A.G. Evans, Acta Metall. Mater. **37**, 917 (1989).
20. S.S. Wong, J.S. Cho, H.K. Kang, and C.H. Ting, *Electronic Packaging Materials Science V*, edited by E.D. Lillie, P.S. Ho, R. Jaccodine, and K. Jackson (Mater. Res. Soc. Symp. Proc. **203**, Pittsburgh, PA, 1991), p. 347.
21. G.G. Stoney, Proc. R. Soc. London Ser. A **82**, 172 (1909).
22. M.E. Thomas, M.P. Hartnett, and J.E. Mckay, J. Vac. Sci. Technol. A **6**, 2570 (1988).
23. R. Abermann, *Thin Films: Stresses and Mechanical Properties III*, edited by W.D. Nix, J.C. Bravman, E. Arzt, and L.B. Freund (Mater. Res. Soc. Symp. Proc. **239**, Pittsburgh, PA, 1992), p. 25.
24. J.A. Ruud, D. Josell, F. Spaepen, and A.L. Greer, J. Mater. Res. **8**, 112 (1993).
25. M. Janda, Thin Solid Films **142**, 37 (1986).
26. R.M. Cannon, R.M. Fisher, and A.G. Evans, *Thin Films—Interfaces and Phenomena*, edited by R.J. Nemanich, P.S. Ho, and S.S. Lau (Mater. Res. Soc. Symp. Proc. **54**, Pittsburgh, PA, 1986), p. 799.
27. J.G. Li, J. Mater. Sci. Lett. **11**, 903 (1992).

APPENDIX

The strain energy release rate

Interfacial decohesion, motivated by residual stresses in deposited thin film layers, occurs subject to the steady-state strain energy release rate, G_{ss}, when the interfacial flaw size, a_0, exceeds the film thickness.[3] Moreover, since the film stress diminishes as the interface decoheres, this energy release behavior is entirely controlled by elasticity, even when the film has yielded upon prior thermal processing.[3] For thin film systems a strain energy balance may be used to calculate G_{ss}, wherein two elements, having width Δa, are chosen far ahead and far behind the growing interfacial crack (Fig. A1). If U_a and U_b denote the strain energies in these volume elements, then

$$G_{ss}\Delta a = U_a - U_b \tag{A1}$$

This result applies provided that the substrate thickness is much larger than the film thickness. The element far ahead of the crack tip is in biaxial plane stress:

$$\begin{aligned} &\sigma_x^i = \sigma_y^i = \sigma_i\,, \\ &\sigma_i = \varepsilon_i E_i/(1-\nu_i) = \varepsilon_i E_i'\,, \\ &\sigma_z^i = \tau_{xy}^i = \tau_{yz}^i = \tau_{zx}^i = 0 \quad (i = 1,2)\,, \end{aligned} \tag{A2}$$

where σ_1, σ_2 are the residual stresses in the two layers and $\varepsilon_1, \varepsilon_2$ the corresponding residual strains. The elastic strain energy density associated with each layer $(i = 1,2)$, per unit width, is

$$\Delta U_a^i/h_i\Delta a = \frac{\sigma_i^2}{E_i'} \tag{A3}$$

where E_i' is the biaxial modulus of the film layers. Consequently, for a bilayer,

$$U_a \equiv \sum \Delta U_a^i = \left[\frac{\sigma_1^2 h_1}{E_1'} + \frac{\sigma_2^2 h_2}{E_2'}\right]\Delta a \tag{A4}$$

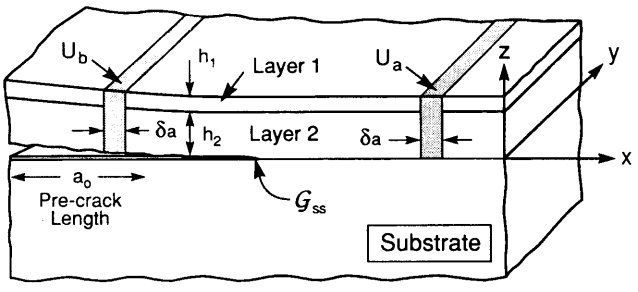

FIG. A1. A schematic describing the energy balance approach to find the strain energy release rate for a bilayer thin film.

When both layers are in residual tension (as in the present experiment) and when $\varepsilon_1 > \varepsilon_2$, the film bends upward after decohesion in an attempt to relax the strains (Fig. 4). The resultant stresses in each layer can be related to the forces, P_i, moments, M_i, and curvature, κ, defined in Fig. 5, by[18]:

$$\begin{aligned} \sigma_i(z) &= P_i/h_i + zE_i'\kappa \\ M_i/I_i &= E_i'\kappa \\ I_i &= h_i^3/12, \end{aligned} \tag{A5}$$

where z now denotes the vertical distance from the neutral axis in each separate layer, whereas I_i is the sectional modulus. The strain energy is then[3]

$$U_b = \sum_i \frac{1}{E_i'}\left[\frac{P_i^2}{h_i} + \frac{M_i^2}{I_i}\right]\Delta a \tag{A6}$$

It is now required to provide expressions that relate P_i, M_i, and κ to the stresses and the film thicknesses, by using beam theory. For a bilayer, this procedure provides five linear equations involving the five unknowns, namely P_1, P_2, M_1, M_2, and κ. Equilibrium dictates that, for a bilayer,

$$\begin{aligned} \sum P_i = 0; &\longrightarrow P_1 = P_2 = P \\ \sum M_i = 0; &\longrightarrow M_1 + M_2 = P\left(\frac{h_1 + h_2}{2}\right) \end{aligned} \tag{A7}$$

Geometry requires that

$$\begin{aligned} M_1 &= E_1'I_1\kappa \\ M_2 &= E_2'I_2\kappa \end{aligned} \tag{A8}$$

Strain compatibility at the interface gives

$$-\varepsilon_1 + \frac{P_1}{E_1'h_1} + \frac{h_1\kappa}{2} = -\varepsilon_2 - \frac{P_2}{E_2'h_2} - \frac{h_2\kappa}{2} \tag{A9}$$

In this case, analytical solutions for P, M_i, and κ are obtained as[18]:

$$\begin{aligned} M_i &= E_i'I_i\kappa \\ P &= \left[\frac{E_1'h_1^3 + E_2'h_2^3}{6(h_1 + h_2)}\right]\kappa \end{aligned}$$

and

$$\kappa = \frac{6(h_1 + h_2)(\varepsilon_1 - \varepsilon_2)}{[h_1^2 + E_2'h_2^3/E_1'h_1 + E_1'h_1^3/E_2'h_2 + h_2^2 + 3(h_1 + h_2)^2]} \tag{A10}$$

The strain energy release rate is then ($i = 1,2$)

$$G_{ss} = \sum_i \frac{\sigma_i^2 h_i}{E_i'} - \sum_i \frac{1}{E_i'}\left[\frac{P^2}{h_i} + \frac{12M_i^2}{h_i^3}\right] \tag{A11}$$

The above result can be generalized for a multilayer film ($i = 1,2,3,\ldots,n$). The number of unknowns is $2n + 1$, because each layer has two (a force, P_i, and a moment, M_i), in addition to the curvature, κ, of the film after decohesion. The solution requires $2n + 1$ linear equations. The first two stem from equilibrium considerations:

$$\sum \text{force} = 0; \longrightarrow P_1 + P_2 + \ldots + P_n = 0 \tag{A12}$$

$$\sum \text{moment} = 0; \longrightarrow \sum_{i=1}^{n} M_i = \sum_{i=1}^{n-1} P_i \times \left(\frac{h_i + h_n}{2} + \sum_{k=i+1}^{n-1} h_k\right) \tag{A13}$$

The next n equations relate the moments to the curvature ($i = 1,2,\ldots,n$)

$$M_i = E_i'I_i\kappa. \tag{A14}$$

Finally, the remaining $n - 1$ equations involve strain compatibility at the $n - 1$ interfaces. For the rth interface from the top, this can be expressed as ($r = 1,2,\ldots,n-1$):

$$\varepsilon_r + \frac{P_r}{E_r'h_r} + \frac{h_r\kappa}{2} = \varepsilon_{r+1} + \frac{P_{r+1}}{E_{r+1}'h_{r+1}} - \frac{h_{r+1}\kappa}{2}. \tag{A15}$$

A program needed to solve these equations has been developed using MATLAB. (The mode mixity may also be calculated.[3] For the present experiments, $\Psi \approx 0°$.)